Neurophysiological oscillatory mechanisms underlying the effect of mirror visual feedback-induced illusion of hand movements on nociception and cortical activation

Marco Rizzo[1], Laura Petrini[1], Claudio Del Percio[2], Lars Arendt-Nielsen[1], and Claudio Babiloni[3]

[1]Aalborg University
[2]Universita La Sapienza
[3]University of Foggia

October 27, 2022

Abstract

Mirror Visual Feedback (MVF)-induced illusion of hand movements produces beneficial effects in patients with chronic pain. However, neurophysiological mechanisms underlying these effects are poorly known. Here we hypothesized that such an MVF-induced movement illusion may exert its effects by changing the activity in midline cortical areas of the pain neural matrix. Electrical stimuli with individually fixed intensity were applied to the left hand in healthy adults to produce painful and non-painful sensations during unilateral right-hand movements with such an MVF illusion and right and bilateral hand movements without MVF. During these events, electroencephalographic (EEG) activity was recorded from 64 scalp electrodes. Event-related desynchronization (ERD) of EEG alpha rhythms (8-12 Hz) indexed the neurophysiological oscillatory mechanisms inducing cortical activation. As compared to the painful sensations, the non-painful sensations were specifically characterized by (1) lower alpha ERD estimated in the cortical midline, angular gyrus, and lateral parietal regions during the experimental condition with MVF and (2) higher alpha ERD estimated in the lateral prefrontal and parietal regions during the control conditions without MVF. These core results suggest that the MVF-induced movement illusion may affect nociception and neurophysiological oscillatory mechanisms reducing the activation in cortical limbic and default mode regions.

Neurophysiological oscillatory mechanisms underlying the effect of mirror visual feedback-induced illusion of hand movements on nociception and cortical activation

[1]Rizzo M., [1]*Petrini L.,[2]Del Percio C., [1,3]Arendt-Nielsen L., and [2,4]Babiloni C.

1 Center for Neuroplasticity and Pain (CNAP), SMI®, Department of Health Science and Technology, Aalborg

University, Aalborg, Denmark

2 Department of Physiology and Pharmacology "V. Erspamer", Sapienza University of Rome, Rome, Italy

3 Department of Medical Gastroenterology, Mech-Sense, Aalborg University Hospital, Aalborg, Denmark

4 Hospital San Raffaele Cassino, Cassino (FR), Italy

Corresponding author: Associate Prof. Laura Petrini

Center for Neuroplasticity and Pain (CNAP)

Department of Health Science and Technology,

The Faculty of Medicine

Aalborg University, Fredrik Bajers Vej 7A/2-201

9220 Aalborg Ø, Denmark

Phone: +45 99 40 98 26

Email: lap@hst.aau.dk

Abstract

Mirror Visual Feedback (MVF)-induced illusion of hand movements produces beneficial effects in patients with chronic pain. However, neurophysiological mechanisms underlying these effects are poorly known. Here we hypothesized that such an MVF-induced movement illusion may exert its effects by changing the activity in midline cortical areas of the pain neural matrix. Electrical stimuli with individually fixed intensity were applied to the left hand in healthy adults to produce painful and non-painful sensations during unilateral right-hand movements with such an MVF illusion and right and bilateral hand movements without MVF. During these events, electroencephalographic (EEG) activity was recorded from 64 scalp electrodes. Event-related desynchronization (ERD) of EEG alpha rhythms (8-12 Hz) indexed the neurophysiological oscillatory mechanisms inducing cortical activation. As compared to the painful sensations, the non-painful sensations were specifically characterized by (1) lower alpha ERD estimated in the cortical midline, angular gyrus, and lateral parietal regions during the experimental condition with MVF and (2) higher alpha ERD estimated in the lateral prefrontal and parietal regions during the control conditions without MVF. These core results suggest that the MVF-induced movement illusion may affect nociception and neurophysiological oscillatory mechanisms reducing the activation in cortical limbic and default mode regions.

1 INTRODUCTION

The illusory phenomenon whereby the mirrored movement of one limb is perceived as the simultaneous movement of the opposite limb is known as Mirror Visual Feedback (MVF) (Ortiz-Catalan et al., 2016; Rjosk et al., 2016). MVF technique entails placing a mirror perpendicularly to the observer's body midline. While watching the limb reflected in the mirror, the observer experiences the misperception of looking at his/her true limb (Ding et al., 2019; Ramachandran & Rodgers-Ramachandran, 1996; Ramachandran, Rogers-Ramachandran, & Cobb, 1995). Several investigations in cohorts of patients with chronic pain or motor deficits demonstrated neuroplasticity processes associated with MVF sensory-motor experience (Arya, 2016; Deconinck et al., 2015). Therefore, MVF-based neurorehabilitation strategies were developed to treat chronic pain conditions, such as phantom limb pain (PLP) syndrome (Finn et al., 2017; Ramachandran et al., 1995; Thøgersen et al., 2020), post-stroke hemiparesis (Bae, Jeong, & Kim, 2012; Bartur, Pratt, Frenkel-Toledo, & Soroker, 2018; Dohle et al., 2009), and complex regional pain syndrome (McCabe et al., 2003; Tichelaar, Geertzen, Keizer, & Paul Van Wilgen, 2007). These strategies were also successful to facilitate upper-extremities motor recovery (Bullock, Won, Bailenson, & Friedman, 2020; Zhang & Fong, 2019).

Neuroimaging studies in healthy individuals used functional magnetic resonance imaging (fMRI) (Merians, Tunik, Fluet, Qiu, & Adamovich, 2009; Numata, Murayama, Takasugi, Monma, & Oga, 2013; Shinoura et al., 2008), near infrared spectrometry (Imai, Takeda, Shiomi, Taniguchi, & Kato, 2008; Inagaki et al., 2019), and transcranial magnetic stimulation (TMS) (Aziz-Zadeh, Maeda, Zaidel, Mazziotta, & Iacoboni, 2002;

Fukumura, Sugawara, Tanabe, Ushiba, & Tomita, 2007; Garry, Loftus, & Summers, 2005) to investigate the brain neural basis of the effects by the MVF procedure. Results showed an MVF-related increase in cortical excitability or activation in premotor, primary motor (M1), and primary somatosensory (S1) cortical areas ipsilateral to the moving hand. Other fMRI and TMS studies extended the focus of the investigation to the whole brain, showing the involvement of the visual and parietal posterior cortical areas – strongly connected with the central sensory-motor regions – as responsible for visuomotor transformation processes occurring during MVF-induced illusory experience (Bartur et al., 2018; Fritzsch et al., 2014; Fukumura et al., 2007; Garry et al., 2005; Hamzei et al., 2012; Matthys et al., 2009; Numata et al., 2013). In this regard, an fMRI study investigated the effects of MVF training in low amputees. After 12 sessions of MVF therapy, patients showed a significant reduction of PLP and increased activity in the bilateral orbitofrontal cortex in response to phantom ankle "imaginary" movement (Seidel et al., 2011). Interestingly, the phantom ankle movements alone induced activation in the premotor and parietal associative cortical areas rather than the primary sensory-motor cortex (Seidel et al., 2011).

The above neuroimaging results had the advantage of a high spatial resolution but were limited in describing the temporal evolution of the MVF-related cortical activation. For this purpose, electroencephalography (EEG) can probe the cortical activity related to motor and sensory events with less spatial resolution but enhanced temporal resolution (milliseconds) (Kim & Lee, 2015; Light et al., 2011). Previous EEG investigations measured lateralized related potentials (as an index of M1 activity) during unilateral hand movement tasks performed with MVF illusion. Those potentials showed clear activation of the M1 contralateral to the hand reflected in the mirror and perceived as moving (indeed immobile) (Debnath & Franz, 2016; Touzalin-Chretien & Dufour, 2008; Touzalin-Chretien, Ehrler, & Dufour, 2010).

Other EEG studies used the so-called event-related desynchronization (ERD) of the cortical EEG alpha (8-12 Hz) rhythms to investigate the neurophysiological oscillatory mechanisms regulating the excitability of the cerebral cortex during sensory and motor events in humans (Neuper, Wörtz, & Pfurtscheller, 2006; Pfurtscheller & Aranibar, 1979; Pfurtscheller & Lopes Da Silva, 1999). Specifically, ample resting-state EEG alpha rhythms reflect the cortical inhibition in the central and posterior sensory-motor areas during a wakefulness state of psychophysical relaxation (Pfurtscheller & Lopes Da Silva, 1999; Pfurtscheller & Neuper, 1994; Babiloni et al., 2020). These alpha rhythms reduce in amplitude (alpha ERD) as a sign of cortical activation during the preparation and execution of voluntary movements (Babiloni et al., 1999, 2014; Neuper et al., 2006; Pfurtscheller & Lopes Da Silva, 1999). Furthermore, central alpha ERD was associated with nociception and sensorimotor interactions (gating) between voluntary hand movements and painful stimuli (Babiloni et al., 2003; 2008, 2010, 2014; Del Percio et al., 2006), while other EEG studies showed consistent alpha ERD overlying frontal and parietal areas during the MVF-induced movement illusion (Bartur et al., 2015; Lee, Li, & Fan, 2015; Rizzo et al., 2022). Altered activity in the frontal and parietal cortical areas was also linked to dysesthesia (i.e., abnormal limb perceptions and emotions associated with pathological pain like PLP) due to MVF-induced sensorimotor incongruence provoked by a mismatch between motor intention and sensory feedback (Foell, Bekrater-Bodmann, Mccabe, & Flor, 2013; Katayama, Osumi, Kodama, & Morioka, 2016; McCabe, Haigh, Halligan, & Blake, 2005). For example, EEG investigations in healthy subjects reported stronger alpha and beta ERD in the bilateral frontal premotor and anterior-posterior cingulate areas when they experienced dysesthesia (Katayama et al., 2019, 2016) and discomfort sensations (Nishigami et al., 2014) induced by the sensorimotor incongruence. Notably, dysesthesia is an interesting experimental model as it is characterized by a discomfort like that reported in people with pathological chronic pain (Daenen et al., 2012; Mccabe, Cohen, & Blake, 2007).

Keeping in mind the above findings, we believe that a methodological approach based on high-resolution EEG and estimation of alpha ERD cortical sources may shed light on the effects of MVF-induced movement illusion on nociception and the activation in the cortical midline (limbic) regions belonging to the so-called pain neural matrix. These cortical midline (limbic) regions including medial prefrontal, anterior and posterior cingulate, and precuneus cortices may underpin human pain experience in relation to the affective sense-of-self, body representation, and interoceptive signals (Araujo, Kaplan, & Damasio, 2013; Babiloni et al., 2003; Cavanna & Trimble, 2006; Goffaux, Girard-Tremblay, Marchand, Daigle, & Whittingstall, 2014; Northoff &

Bermpohl, 2004; Northoff et al., 2006). In this line, here we tested the hypothesis that in healthy adults, the MVF-related illusion of hand movements may affect the nociception and the activation in the midline cortical areas, as revealed by the alpha ERD. To test this hypothesis, electrical stimuli were applied to the left hand to produce painful or non-painful sensations during unilateral right-hand movements with MVF. As control conditions, the same electrical stimuli were applied during unilateral right-hand and bilateral hand movements without MVF. The alpha ERD was estimated within mathematical sources modelled in the cortical midline and control regions.

2 MATERIALS AND METHODS

2.1 Subjects

Thirteen healthy adult volunteers were recruited for the study (mean age = 26.2, SD = ±4.7). The main exclusion criteria included the presence of chronic pain, nerve pain, neurological diseases, current medical treatments, and participation in other studies involving pain stimulation in the past four weeks. The Edinburgh Handedness Inventory (EHI, Oldfield, 1971) confirmed that all the subjects were right-handed. Remarkably, ten subjects participated in our previous MVF study (Rizzo et al., 2022). All experiments were conducted at the Aalborg University (Denmark). The study was approved by the Scientific Ethical Committee of Region Nordjylland (N-20190008) and all participants signed the informed consent according to the Declaration of Helsinki.

2.2 Experimental procedure

The participants were comfortably seated on a chair with their arms lying symmetrically ahead on a table. Auditory cues of 70 dB, 1000 Hz, and 50 ms of duration (Kida et al., 2006) were used to trigger right index finger movements. Three different conditions (80 trials each) were randomized across the participants. In the experimental condition (Unilateral with Mirror, or UM+) the mirror was placed on the desk, perpendicularly to the subjects' midsagittal plane with the reflecting face on the right side (Figure 1). Subjects were instructed to move the right index finger in response to the auditory cue while watching the image of the reflected moving hand in the mirror to give the illusion of the simultaneous left index finger movement. The position of the left hand behind the mirror corresponded to the image of the left hand reflected in the mirror. In the control conditions, the mirror was removed from the experimental setting and the left hand was directly visible to the participants. In one control condition (Unilateral without Mirror, UM-), subjects were asked to perform the same unilateral right index finger movements. In the other control condition (Bilateral without Mirror, BM-), subjects had to perform synchronous movements of both index fingers. The movements consisted of a double extension of the index finger with a slow release toward the bottom (approx. 1 s). All the participants received a brief training to perform the movement correctly and keep the left hand as still as possible during the unilateral conditions. In each condition, an electrical stimulus was delivered on the tip of the left index finger 100 ms after the auditory cue to induce cortical sensory-motor interaction (Figure 2). The interval between the stimuli was fixed at 10 s, a sufficient period to reset the desynchronization of the alpha rhythms (Babiloni et al., 2008). A fixed interval also allowed to produce a sort of predictability of the upcoming auditory and electrical stimuli, optimal to study the anticipatory alpha ERD/ERS responses. However, subjects were not informed of this fixed interval to avoid any counting strategies.

2.3 Electrical stimulations and pain threshold detection

Electrical stimulations were provided by a voltage-controlled current stimulator (NoxiSTIM; JNI Biomedical; Aalborg, Denmark). Stimuli were delivered on the tip of the left finger using an electrode with a gold pin cathode and a ring anode (Figure 1). An inactive electrode (sham) was placed on the right index finger to achieve a congruent mirror visual feedback (Figure 1). A multi-channel data acquisition module (NI-6221, National Instruments Corp., Austin, TX, USA) was used to synchronize the electrical stimuli to the auditory cues.

Subjects were asked to evaluate the intensity of electrical stimuli using a Numerical Scale Rating (NRS) from 0 to 10, where 0 represents the absence of any sensory perception, whereas 10 is the "worst imaginable pain".

Before the pain threshold measurement, 15 stimuli at random intensities were delivered in a familiarization phase. The method of limits was used to determine the pain threshold for each subject. Starting from 0.5 milliamperes (mA), the current intensity was progressively increased until a rating of 5 out of 10, namely the minimum current intensity producing a painful sensation (Hu, Cai, Xiao, Luo, & Iannetti, 2014). The fixed individual pain threshold was used during the three conditions (mean mA = 5.5; SD = ± 3.1). During the experiment, subjects were asked to provide a numerical value (decimals included) of the average pain intensity of the last 5 trials. Since each condition consisted of 80 trials, 16 values per condition were considered in the analysis. Due to the fluctuant subjective perception of fixed stimuli, painful (NRS > 5) and non-painful (NRS < 5) responses were obtained for each condition. If one condition did not show that fluctuation in the perceived pain intensity, the single dataset was removed from the analysis. Therefore, the final samples considered in the statistical analysis were: UM+ = 8 subjects, UM- = 13 subjects, and BM- = 12 subjects. Of interest, the painful epochs (NRS > 5) were 36.5% in the UM- condition, 58.5% in the BM- condition, and 53.9% in the UM+ condition.

2.3 EEG recording and analysis

The EEG activity was recorded from scalp electrodes by an active 64-channels system (g.HIamp amplifier, g.tec medical engineering GmbH, Austria) according to the 10-10 international system. Ground and reference electrodes were placed on the forehead and ear lobes, respectively. The electrode impedance was kept under 5 k and the sampling rate was 1200 Hz. Eye movements and blinking activity was controlled by Fp1 and Fp2 channels (Zeng et al., 2013). The offline data analysis was performed using the EEGLAB 2021.1 (Delorme & Makeig, 2004) freeware toolbox for MatLab R2018b (MathWorks, Inc., Natick, MA, USA). After visual inspection, data were filtered with a zero-phase basic FIR filter (0.3-40 Hz), resampled to 256 Hz, re-referenced, and epoched in 80-time windows of 9 s each. Artefacts, such as blinking, muscular movements, 50 Hz noise, etc., were recognized and removed using the Infomax independent component analysis (ICA) algorithm (Bell & Sejnowski, 1995). On percentage, 7.9% of artefact epochs and 7.3% of artefact components were removed from the EEG datasets. Finally, to quantify the alpha ERD/ERS from the artefact-free EEG epochs, the global EEG spectrum was computed using an FFT-based method. The outcomes were used to select the individual alpha frequency peak (IAFp) from the EEG power spectra. IAFp was defined as the frequency showing the highest peak within the alpha band (8-12 Hz) (Klimesch, 1999). Thus, the EEG data were individually filtered at the alpha frequency band depending on the IAFp, namely from IAFp-2 Hz to IAFp+2 Hz (mean IAFp = 10.1; SD = +- 1.0).

2.4 Cortical sources estimation

The freeware tool "exact Low-Resolution Brain Electromagnetic Tomography" (eLORETA) (Pascual-Marqui, 2007) used artifact-free EEG data as input for the cortical source estimation. The eLORETA freeware is a functional imaging technique belonging to a family of standardized linear inverse solution procedures modelling the 3D distributions of the EEG sources within a head volume conductor model comparted in the scalp, skull, and brain (Pascual-Marqui, Esslen, Kochi, & Lehmann, 2002; Pascual-Marqui et al., 1999). eLORETA solves the EEG inverse problem by estimating the current density values at the voxel level and provides a brain source space restricted to the cortical grey matter of 6,239 voxels (5 mm resolution, with each voxel containing an equivalent current dipole), as based on the Montreal Neurological Institute template (MNI152). For each voxel, eLORETA provides information about the MNI coordinates, the lobe, and the Brodmann area (BA). The input for the source estimation was the spectral power density computed by 62 scalp electrodes as eLORETA source analysis is a free-reference method (W. Peng, Hu, Mao, & Babiloni, 2015), (i.e., the two reference electrodes were not considered in the analysis). Due to the low spatial resolution characteristic of the EEG techniques, adjacent Brodmann areas were clusterized. The clusters included BAs 1-2-3 together with BA 4 (sensory-motor area), BA 24 together with BA 32 (anterior cingulate cortex), BA 44 with BA 45 (inferior frontal gyrus), and BA 9 with BA 46 (superior frontal gyrus or dorsolateral prefrontal cortex).

2.5 Alpha ERD/ERS calculation

Standard quantification of the alpha ERD/ERS was performed for the anticipation and execution stages of the movements (Babiloni et al., 2010; Pfurtscheller & Aranibar, 1979; Pfurtscheller & Lopes Da Silva, 1999; Pfurtscheller & Neuper, 1994; Pfurtscheller et al., 1997). The alpha ERD/ERS was calculated by the following formula: ERD/ERS% = (E-R)/R*100, where E and R represent the power density at the "Event" (1 s) and "Rest" (1 s) periods. The "Rest" was defined as the period from 5 s to 4 s before the auditory cues triggering the movement. The anticipation "Event" was defined as the period of 1 s before the auditory cues. Finally, the execution "Event" was defined as the period of 1 s from 250 ms to 1250 ms after the auditory cues and the alpha ERD peak within this interval was considered in the analysis. The first 250 ms after the auditory cues were intentionally removed to exclude the auditory-evoked potentials (N1-P2 complex) (Lightfoot, 2016) and the pain-evoked potentials (N2-P2 complex) (Babiloni et al., 2008; Fabrizi et al., 2016; Mouraux, Iannetti, & Plaghki, 2010). The resulting negative percentage values represented the alpha ERD, as a reflection of cortical activity. On the contrary, positive percentage values represented the alpha ERS as a reflection of cortical inhibition (Pfurtscheller & Lopes Da Silva, 1999; Pfurtscheller et al., 1997). For the scalp analysis, clusters of electrodes were considered for each hemisphere at frontal (F3 and FC3; F4 and FC4) and centro-parietal (C3, CP3, and P3; C4, CP4, and P4) levels. On the other hand, the eLORETA solutions were used to compute the cortical voxel-level ERD/ERS in the alpha frequency band.

2.6 Statistical analysis for the ERD/ERS scalp distribution

Linear mixed model for repeated measures was used to assess whether the subjective perception of the stimulus intensity was depending on the MVF. The fixed factors were *Condition* (UM+, UM-, and BM-) and*Stimulus* (pain and no-pain), whereas the random factor was the number of subjects in each group. The models were fitted separately in the left and right hemispheres for the frontal (F3-FC3 and F4-FC4) and centro-parietal (C3-CP3-P3 and C4-CP4-P4) clusters of electrodes as well as for the anticipation and execution phases of the event. The linear mixed model statistical analysis was carried out using IBM SPSS Statistics 27 (IBM, New York, USA).

2.7 Statistical analysis for the alpha ERD/ERS cortical sources

To investigate the differences in the cortical activation between stimuli perceived as painful and non-painful, statistical nonparametric mapping voxel-based wise randomization tests (5000 permutations) were applied for the alpha ERD/ERS eLORETA solutions for each condition (UM+, UM-, and BM-) and stage of the event (Anticipation and Execution). The outcomes obtained through this statistical approach are equivalent to statistical parametric methods with multiple comparison corrections (Nichols & Holmes 2001). This nonparametric permutation is particularly useful when analyzing small sample sizes with low degrees of freedom (Bian et al., 2019; Nichols & Holmes, 2001). The results are displayed as voxel-by-voxel T statistics maps with a corrected $P < 0.05$ (randomization tests correction) (Nichols & Holmes, 2001). To weaken the type II error (risk of false negatives), an uncorrected significance threshold of a more severe $P < 0.001$ was also considered in the analysis. Only cortical areas with a minimum number of 5 voxels were considered in the analysis. These statistical analyses were performed using eLORETA statistical toolbox (Pascual-Marqui, 2007).

2.8 Control analysis

Event-related potentials (ERPs) in response to the auditory cues and electrical stimuli were extracted from the Cz electrode. Successively, the waveforms resulting from painful and non-painful blocks were averaged across the subjects for each condition and paired samples t-tests were used for statistical comparison. The ERPs considered were the N1-P2 (auditory), P2-N2 complex (electrical stimulus), and P3 (attentional). Furthermore, the randomness of the painful and non-painful epochs was tested by performing the RUNS test for each subject and condition. Finally, NRS values were compared in order to control differences in the subjective perception of the stimulus intensity for each condition. All the statistical analyses were performed using IBM SPSS Statistics 27 (IBM, New York, USA).

3 *RESULTS*

3.1 Scalp topography

Figure 3 shows the scalp distribution of the alpha ERD/ERS for the three conditions (UM-, BM-, and UM+) at the anticipation (1000 ms before the auditory cue) and execution (peak within 1250 ms after the auditory cue) of the event. The cortical activity patterns resulting from the blocks perceived as painful (NRS > 5) and non-painful (NRS < 5) are thus compared. In the control conditions without MVF (UM- and BM-), results indicate similar centrally-distributed alpha ERD in the anticipation phase of the event. When considering the execution phase, the alpha ERD is stronger and more widespread in the non-painful than painful blocks in both conditions. In the experimental MVF condition, the alpha ERD shows an opposite activity pattern, i.e., stronger in the painful than non-painful blocks. Moreover, it shows a prominent parieto-central distribution. Even in the MVF condition, the alpha ERD is stronger and more widespread during the execution phase of the event.

However, the linear mixed model analyses performed to assess the interaction between the stimulus intensities and the conditions did not indicate any statistically significant effect neither for the frontal nor central brain regions (p > 0.05).

3.2 Control conditions without MVF

This section of the results considers the differences between painful and non-painful blocks for the control conditions without the MVF illusion (i.e., UM- and BM-). The spatial distribution of the p values related to the Student's t-tests (parametric statistical maps) for the eLORETA solutions of the alpha ERD/ERS is illustrated in Figure 4 (first and second rows). The significant T values with the relative voxel cluster size and locations are listed in Table 1.

For both conditions, the anticipation and execution phases of the event are characterized by a stronger activation (alpha ERD) in the non-painful than painful blocks. In particular, the UM- condition shows this pattern in the left anterior cingulate (BA 32; peak value: T = 4.36; p < 0.05 corrected) and inferior parietal cortex (BA 40; peak value: T = 3.95; p < 0.05 corrected) in the anticipatory phase, and no significant differences in the execution phase. In the BM- conditions, the differences appear in the bilateral sensory-motor (BAs 1-2-3, 4; peak value: 4.61; p < 0.05 corrected), inferior parietal (BA 40; peak value: T = 4.46; p < 0.05) cortical areas, and bilateral inferior frontal gyrus (BAs 44-35; peak value: T = 3.36; p < 0.001 uncorrected), for the anticipation phase. Furthermore, the execution phase of the event shows those differences in the right superior (BAs 9-46; peak value: T = 4.11; p < 0.05 corrected) and inferior (BAs 44-45; peak value: T = 3.79; p < 0.001 uncorrected) frontal gyri as well as right anterior cingulate cortex (BA 32; peak value: T = 3.67; p < 0.001 uncorrected).

3.3 Experimental condition with MVF

The results from the voxel-by-voxel comparisons between painful and non-painful blocks in the experimental MVF (UM+) condition are hereby reported. The spatial distribution of the P values related to the Student's t-tests is illustrated in Figure 4 (bottom). All the significant T values with the relative voxels cluster size and localizations are summarized in Table 1.

Unlike the control conditions, in the UM+ condition, the alpha ERD observed in the painful blocks was stronger than the alpha ERD in the non-painful blocks. During the anticipation phase, the main differences are observed in the right posterior cingulate (BA 30; peak value: T = -4.16; p < 0.05 corrected) and the inferior posterior parietal cortex (BA 40; peak value: T = -4.73; p < 0.05 corrected). During the execution phase, these differences are widespread in the frontal and posterior areas. In particular, results showed significant differences in the right polar frontal (BA 10; peak value: T = -4.31; p < 0.05 corrected) and inferior posterior parietal (BA 40; peal value: T = -4.67; p < 0.05 corrected) cortical areas. The same was true in the right middle temporal gyrus (BA 39; peak value: T = -4.75; p < 0.05 corrected) and precuneus (BA 19; peak value: T = -3.87; p < 0.001 uncorrected) as well as in the bilateral anterior cingulate (BAs 24-32; peak value: T = -4.66; p < 0.05 corrected).

3.4 Control analysis

The ERP waveforms are plotted in Fig. 5. Results indicate as the negative peaks (N1 and N2) present higher amplitude in the painful (red line) than non-painful (black line) blocks. This was true at a statistical level for the N1 in the UM+ condition ($p < 0.05$) as well as for the N2 in the UM- condition ($p < 0.05$). Moreover, the P2 peak showed higher amplitude in the painful than non-painful blocks in the UM+ condition ($p < 0.05$). Interestingly, no differences were observed for the attentional P3 ERP. No statistically significant differences were found in the latency measures.

The RUNS test's results for the experimental condition (UM+) showed no significant differences (average number of Runs = 6.8; SD = +- 1.6; $p > 0.05$) (Figure 6), indicating that the order of the blocks in which the subjects perceived the electrical stimuli as painful or non-painful presents a random distribution (i.e., the variability in the individual perceived intensity was not due to habituation or sensitization effects).

Finally, paired samples t-tests showed that NRS values relative to painful blocks are significantly higher than values in the non-painful blocks for each condition ($p < 0.001$ for all comparisons) (Figure 7).

4 DISCUSSION

In the present exploratory study, we hypothesized that the MVF-induced illusion of hand movements may affect the nociception and the activation in the cortical midline areas of the pain neural matrix. For this purpose, we used an original methodological approach. Electrical stimuli at about the pain threshold were applied to the left hand to produce painful or non-painful sensations during unilateral right-hand movements with the MVF and, as control conditions, during unilateral right and bilateral hand movements without the MVF. The eLORETA freeware estimated the EEG source activity, and the alpha ERD (as a sign of cortical activation) reflected the neurophysiological oscillatory mechanisms underlying the painful and non-painful sensations associated with the MVF-related movement illusion.

The results of a control analysis showed that the vertex N1-P2 and/or N2 peaks of the sensory evoked potentials exhibited higher amplitude in relation to the painful over the non-painful sensations during both MVF and noMVF conditions. These results corroborate the reliability of the participants' subjective sensations, in line with previous studies demonstrating that those sensory-evoked potentials can be considered trustworthy neurophysiological signatures of enhanced cortical arousal and pain experience in humans (Fabrizi et al., 2016; Lightfoot, 2016; Mouraux et al., 2010).

The core results of the present study showed that as compared to the painful sensations, the non-painful sensations during the MVF condition were specifically characterized by lower alpha ERD (cortical activation) estimated in the right cortical midline regions (i.e., medial prefrontal, anterior and posterior cingulate, parietal cortex, and precuneus), angular gyrus, and inferior parietal lobule contralateral to the electric hand stimulation and ipsilateral to the hand movements. In contrast, the non-painful sensations during the control noMVF conditions were specifically characterized by stronger alpha ERD estimated in the left lateral prefrontal and inferior parietal lobule regions ipsilateral to the electric hand stimulation and contralateral to the hand movements. The functional meaning of these results is discussed in the following sections.

4.1 The effects of the MVF-induced movement illusion on the cortical activity and pain

During the MVF condition, the non-painful over painful sensations were specifically related to lower alpha ERD in the right cortical midline regions of the limbic and default mode network, in the right angular gyrus of the default mode network, and the right inferior parietal lobule of the ventral attention network. In contrast, the non-painful sensations in the noMVF conditions were characterized by higher alpha ERD in the left lateral prefrontal and inferior parietal lobule of the ventral attention networks.

The present results emphasize the role of brain neurophysiological oscillatory mechanisms operating at alpha frequencies for modulating the de -activation of the above cortical regions relevant to human nociception. In this regard, they complement the following previous neuroimaging findings obtained in humans: (1) the involvement of medial prefrontal and anterior-posterior cingulate cortices in processing the affective component of pain (Peng, Steele, Becerra, & Borsook, 2018; Tolomeo et al., 2016); (2) the activation of cortical midline regions in association with the unpleasantness sensations induced by painful stimuli (De Ridder &

8

Vanneste, 2016; Kulkarni et al., 2005; Price, 2000); and (3) the activation of a posterior cortical subnetwork encompassing inferior parietal lobe, posterior cingulate cortex, and precuneus related to affective and cognitive components (i.e., the expectation of pain and self-awareness) of the pain experience (Fauchon et al., 2019). Moreover, the present results complement previous evidence showing that experimental sensorimotor incongruence in healthy individuals may induce alteration in limb perceptions and emotions (dysesthesia) (Foell, Bekrater-Bodmann, Mccabe, & Flor, 2013; Katayama, Osumi, Kodama, & Morioka, 2016; McCabe, Haigh, Halligan, & Blake, 2005; Nishigami et al., 2014). In these studies, dysesthesia was linked to abnormal EEG alpha and beta rhythms desynchronization estimated in parietal, midline premotor, and cingulate cortical areas (Katayama et al., 2019, 2016; Nishigami et al., 2014). Notably, such discomfort is similar to that reported in people with pathological chronic pain (Daenen et al., 2012; Mccabe et al., 2007).

Taken together, the present and the aforementioned neuroimaging findings inspired the following speculation. In the present MVF condition, the reduced alpha ERD in the right cortical midline limbic regions may be related to non-painful sensations concerning attenuated affective sense-of-self and internal body perception (Araujo et al., 2013; Katayama et al., 2016; Nishigami et al., 2014; Northoff & Bermpohl, 2004; Northoff et al., 2006). Furthermore, the reduced alpha ERD in the right default mode network regions may be associated with attenuated body-related (interoceptive) internal representations (Broyd et al., 2009; Gusnard & Raichle, 2001; Raichle et al., 2001). In contrast, in the present noMVF conditions, the increased alpha ERD in the left lateral prefrontal and inferior parietal lobule may be related to non-painful sensations in relation to a significant allocation of the attention and cognitive states on the true moving hand(s) for "body gnosis," with interferential effects on the neural signals induced by the electric hand stimulation (Rusconi, Pinel, Dehaene, & Kleinschmidt, 2010; Rusconi, Walsh, & Butterworth, 2005). Unfortunately, EEG techniques do not have the fine spatial resolution necessary to disentangle the different subcomponents of a given midline cortical region belonging to either the limbic or default mode network.

During the present MVF condition, the participants may experience the self-oriented attentional and cognitive states associated with the illusory sense of ownership ("the illusory moving hand belongs to my body") and agency ("I am moving the hand reflected in the mirror") for the moving hand reflected in the mirror. According to previous alpha ERD evidence from our group (Rizzo et al., 2022), these states may be related to the activation of lateral prefrontal, premotor, and parietal cortical regions in the hemisphere ipsilateral to the true unilateral hand movements and contralateral to the moving hand reflected in the mirror. Notably, in the present experiments, the only region of that cortical network showing an effect related to pain was the left inferior parietal lobule. Specifically, the non-painful over painful sensations during the MVF condition were associated with lower alpha ERD in the right inferior parietal lobule, as opposed to the higher alpha ERD in the left inferior parietal lobule during the noMVF conditions. It can be speculated that during the MVF condition, the non-painful sensations were also related to a low activation in the right lateral parietal area integrating the visual-somato(nociceptive)-motor information regarding the electrically stimulated left hand.

Future multimodal EEG-fMRI studies should shed light on the effects of the MVF-related movement illusion on the nociception and the functional connectivity between all cortical and subcortical (e.g., amygdala-hypothalamus, amygdala-septum, hippocampus-mammillary bodies, etc.) components of the limbic system. A modulation in this connectivity is expected to impact the integration of primary needs, the emotional value of the painful stimuli, and interoceptive signals related to the persons' experience in relation to the wellness-illness axis during painful stimulations (Cavanna & Trimble, 2006; Goffaux et al., 2014; Northoff & Bermpohl, 2004). Furthermore, future studies may investigate the functional connectivity between the limbic and the default mode networks in connection with the MVF effects on nociception.

5 CONCLUSIONS

Here we hypothesized that in healthy adults, an MVF-induced movement illusion may exert its effects changing the activation in midline cortical areas of the pain neural matrix through neurophysiological oscillatory mechanisms revealed by EEG alpha rhythms.

As compared to the painful sensations, the non-painful sensations were specifically characterized by (1) lower alpha ERD (mathematically) estimated in the cortical midline, angular gyrus, and lateral parietal regions during the experimental condition with MVF and (2) higher alpha ERD estimated in the lateral prefrontal and parietal regions during the control conditions without MVF.

These core results suggest that the MVF-induced movement illusion may affect nociception and neurophysiological oscillatory mechanisms reducing the activation in cortical limbic and default mode regions that may attenuate the affective sense-of-self, internal body perception, body-related (interoceptive) internal representations, and attention to signals triggered by the electrically stimulated left hand.

Conflicts of interest

The authors have no conflicts of interest to declare.

Data availability statement

The data that support the findings of this study are available on request from the corresponding author, MR. The data are not publicly available due to their confidential contents that could compromise the privacy of research participants.

References

Araujo, H. F., Kaplan, J., & Damasio, A. (2013). Cortical midline structures and autobiographical-self processes: An activation-likelihood estimation meta-analysis. *Frontiers in Human Neuroscience* ,*7* (SEP), 1–10. https://doi.org/10.3389/fnhum.2013.00548

Arya, K. N. (2016). Underlying neural mechanisms of mirror therapy: Implications for motor rehabilitation in stroke. *Neurology India* ,*64* (1), 38–44. https://doi.org/10.4103/0028-3886.173622

Aziz-Zadeh, L., Maeda, F., Zaidel, E., Mazziotta, J., & Iacoboni, M. (2002). Lateralization in motor facilitation during action observation: A TMS study. *Experimental Brain Research* , *144* (1), 127–131. https://doi.org/10.1007/s00221-002-1037-5

Babiloni, C., Barry, R. J., Başar, E., Blinowska, K. J., Cichocki, A., Drinkenburg, W. H. I. M., . . . Hallett, M. (2020). International Federation of Clinical Neurophysiology (IFCN) – EEG research workgroup: Recommendations on frequency and topographic analysis of resting state EEG rhythms. Part 1: Applications in clinical research studies.*Clinical Neurophysiology* , *131* (1), 285–307. https://doi.org/10.1016/j.clinph.2019.06.234

Babiloni, C., Brancucci, A., Babiloni, F., Capotosto, P., Carducci, F., Cincotti, F., . . . Rossini, P. M. (2003). Anticipatory cortical responses during the expectancy of a predictable painful stimulation. A high-resolution electroencephalography study. *European Journal of Neuroscience* , *18* (6), 1692–1700. https://doi.org/10.1046/j.1460-9568.2003.02851.x

Babiloni, C., Capotosto, P., Brancucci, A., Del Percio, C., Petrini, L., Buttiglione, M., . . . Arendt-Nielsen, L. (2008). Cortical Alpha Rhythms Are Related to the Anticipation of Sensorimotor Interaction Between Painful Stimuli and Movements: A High-Resolution EEG Study.*Journal of Pain* , *9* (10), 902–911. https://doi.org/10.1016/j.jpain.2008.05.007

Babiloni, C., Capotosto, P., Del Percio, C., Babiloni, F., Petrini, L., Buttiglione, M., . . . Rossini, P. M. (2010). Sensorimotor interaction between somatosensory painful stimuli and motor sequences affects both anticipatory alpha rhythms and behavior as a function of the event side. *Brain Research Bulletin* , *81* (4–5), 398–405. https://doi.org/10.1016/j.brainresbull.2009.11.009

Babiloni, C., Carducci, F., Cincotti, F., Rossini, P. M., Neuper, C., Pfurtscheller, G., & Babiloni, F. (1999). Human movement-related potentials vs desynchronization of EEG alpha rhythm: A high-resolution EEG study. *NeuroImage* , *10* (6), 658–665. https://doi.org/10.1006/nimg.1999.0504

Babiloni, C., Del Percio, C., Arendt-Nielsen, L., Soricelli, A., Romani, G. L., Rossini, P. M., & Capotosto, P. (2014). Cortical EEG alpha rhythms reflect task-specific somatosensory and motor interactions in humans.

Clinical Neurophysiology , *125* (10), 1936–1945. https://doi.org/10.1016/j.clinph.2014.04.021

Bae, S. H., Jeong, W. S., & Kim, K. Y. (2012). Effects of mirror therapy on subacute stroke patients' brain waves and upper extremity functions. *Journal of Physical Therapy Science* , *24* (11), 1119–1122. https://doi.org/10.1589/jpts.24.1119

Bartur, G., Pratt, H., Dickstein, R., Frenkel-Toledo, S., Geva, A., & Soroker, N. (2015). Electrophysiological manifestations of mirror visual feedback during manual movement. *Brain Research* , *1606* , 113–124. https://doi.org/10.1016/j.brainres.2015.02.029

Bartur, G., Pratt, H., Frenkel-Toledo, S., & Soroker, N. (2018). Neurophysiological effects of mirror visual feedback in stroke patients with unilateral hemispheric damage. *Brain Research* , *1700* , 170–180. https://doi.org/10.1016/j.brainres.2018.09.003

Bell, A., & Sejnowski, T. (1995). An Informatio-Maximization Approach to Blind Separation and Blind Deconvolution. *Neural Computation* ,*7* , 1129–1159.

Bian, Y., Qi, H., Zhao, L., Ming, D., Guo, T., & Fu, X. (2019). Dynamic visual guidance with complex task improves intracortical source activities during motor imagery. *NeuroReport* , *30* (9), 645–652. https://doi.org/10.1097/WNR.0000000000001251

Broyd, S. J., Demanuele, C., Debener, S., Helps, S. K., James, C. J., & Sonuga-Barke, E. J. S. (2009). Default-mode brain dysfunction in mental disorders: A systematic review. *Neuroscience and Biobehavioral Reviews* , *33* (3), 279–296. https://doi.org/10.1016/j.neubiorev.2008.09.002

Bullock, K., Won, A. S., Bailenson, J., & Friedman, R. (2020). Virtual Reality-Delivered Mirror Visual Feedback and Exposure Therapy for FND: A Midpoint Report of a Randomized Controlled Feasibility Study.*Journal of Neuropsychiatry and Clinical Neuroscience* , *32* , 90–94.

Cavanna, A. E., & Trimble, M. R. (2006). The precuneus: A review of its functional anatomy and behavioural correlates. *Brain* ,*129* (3), 564–583. https://doi.org/10.1093/brain/awl004

Daenen, L., Nijs, J., Roussel, N., Wouters, K., Van loo, M., & Cras, P. (2012). Sensorimotor incongruence exacerbates symptoms in patients with chronic whiplash associated disorders: An experimental study.*Rheumatology (United Kingdom)* , *51* (8), 1492–1499. https://doi.org/10.1093/rheumatology/kes050

De Ridder, D., & Vanneste, S. (2016). Burst and tonic spinal cord stimulation: Different and common brain mechanisms.*Neuromodulation* , *19* (1), 47–59. https://doi.org/10.1111/ner.12368

Debnath, R., & Franz, E. A. (2016). Perception of hand movement by mirror reflection evokes brain activation in the motor cortex contralateral to a non-moving hand. *Cortex* , *81* , 118–125. https://doi.org/10.1016/j.cortex.2016.04.015

Deconinck, F. J. A., Smorenburg, A. R. P., Benham, A., Ledebt, A., Feltham, M. G., & Savelsbergh, G. J. P. (2015). Reflections on mirror therapy: A systematic review of the effect of mirror visual feedback on the brain. *Neurorehabilitation and Neural Repair* , *29* (4), 349–361. https://doi.org/10.1177/1545968314546134

Delorme, A., & Makeig, S. (2004). EEGLAB: An open source toolbox for analysis of single-trial EEG dynamics including independent component analysis. *Journal of Neuroscience Methods* , *134* (1), 9–21. https://doi.org/10.1016/j.jneumeth.2003.10.009

Ding, L., Wang, X., Guo, X., Chen, S., Wang, H., Cui, X., . . . Jia, J. (2019). Effects of camera-based mirror visual feedback therapy for patients who had a stroke and the neural mechanisms involved: Protocol of a multicentre randomised control study. *BMJ Open* , *9* (3). https://doi.org/10.1136/bmjopen-2018-022828

Dohle, C., Püllen, J., Nakaten, A., Küst, J., Rietz, C., & Karbe, H. (2009). Mirror therapy promotes recovery from severe hemiparesis: A randomized controlled trial. *Neurorehabilitation and Neural Repair* , *23* (3), 209–217. https://doi.org/10.1177/1545968308324786

Fabrizi, L., Verriotis, M., Williams, G., Lee, A., Meek, J., Olhede, S., & Fitzgerald, M. (2016). Encoding of mechanical nociception differs in the adult and infant brain. *Scientific Reports* , *6* (28642), 1–10. https://doi.org/https://doi.org/10.1038/srep28642

Fauchon, C., Faillenot, I., Quesada, C., Meunier, D., Chouchou, F., Garcia-Larrea, L., & Peyron, R. (2019). Brain activity sustaining the modulation of pain by empathetic comments. *Scientific Reports* ,*9* (1), 1–10. https://doi.org/10.1038/s41598-019-44879-9

Finn, S. B., Perry, B. N., Clasing, J. E., Walters, L. S., Jarzombek, S. L., Curran, S., . . . Tsao, J. W. (2017). A randomized, controlled trial of mirror therapy for upper extremity phantom limb pain in male amputees. *Frontiers in Neurology* , *8* (JUL), 1–7. https://doi.org/10.3389/fneur.2017.00267

Foell, J., Bekrater-Bodmann, R., Mccabe, C. S., & Flor, H. (2013). Sensorimotor incongruence and body perception: An experimental investigation. *Frontiers in Human Neuroscience* , *7* (JUN), 1–9. https://doi.org/10.3389/fnhum.2013.00310

Fritzsch, C., Wang, J., Dos Santos, L. F., Mauritz, K. H., Brunetti, M., & Dohle, C. (2014). Different effects of the mirror illusion on motor and somatosensory processing. *Restorative Neurology and Neuroscience* , *32* (2), 269–280. https://doi.org/10.3233/RNN-130343

Fukumura, K., Sugawara, K., Tanabe, S., Ushiba, J., & Tomita, Y. (2007). Influence of mirror therapy on human motor cortex.*International Journal of Neuroscience* , *117* (7), 1039–1048. https://doi.org/10.1080/00207450600936841

Garry, M. I., Loftus, A., & Summers, J. J. (2005). Mirror, mirror on the wall: Viewing a mirror reflection of unilateral hand movements facilitates ipsilateral M1 excitability. *Experimental Brain Research* , *163* (1), 118–122. https://doi.org/10.1007/s00221-005-2226-9

Goffaux, P., Girard-Tremblay, L., Marchand, S., Daigle, K., & Whittingstall, K. (2014). Individual Differences in Pain Sensitivity Vary as a Function of Precuneus Reactivity. *Brain Topography* ,*27* , 366–374. https://doi.org/DOI: 10.1007/s10548-013-0291-0

Gusnard, D., & Raichle, M. (2001). Searching for a baseline: functional imaging and the resting human brain. *Nature Reviews Neuroscience* ,*2* (October), 685–694. https://doi.org/10.1038/35094500

Hamzei, F., Läppchen, C. H., Glauche, V., Mader, I., Rijntjes, M., & Weiller, C. (2012). Functional plasticity induced by mirror training: The mirror as the element connecting both hands to one hemisphere.*Neurorehabilitation and Neural Repair* , *26* (5), 484–496. https://doi.org/10.1177/1545968311427917

Hu, L., Cai, M. M., Xiao, P., Luo, F., & Iannetti, G. D. (2014). Human brain responses to concomitant stimulation of Aδ and C nociceptors.*Journal of Neuroscience* , *34* (34), 11439–11451. https://doi.org/10.1523/JNEUROSCI.1355-14.2014

Imai, I., Takeda, K., Shiomi, T., Taniguchi, T., & Kato, H. (2008). Sensorimotor cortex activation during mirror therapy in healthy right-handed subjects: A study with near-infrared spectroscopy.*Journal of Physical Therapy Science* , *20* (2), 141–145. https://doi.org/10.1589/jpts.20.141

Inagaki, Y., Seki, K., Makino, H., Matsuo, Y., Miyamoto, T., & Ikoma, K. (2019). Exploring hemodynamic responses using mirror visual feedback with electromyogram-triggered stimulation and functional near-infrared spectroscopy. *Frontiers in Human Neuroscience* ,*13* (February), 1–8. https://doi.org/10.3389/fnhum.2019.00060

Katayama, O., Nishi, Y., Osumi, M., Takamura, Y., Kodama, T., & Morioka, S. (2019). Neural activities behind the influence of sensorimotor incongruence on dysesthesia and motor control.*Neuroscience Letters* , *698* (January), 19–26. https://doi.org/10.1016/j.neulet.2019.01.010

Katayama, O., Osumi, M., Kodama, T., & Morioka, S. (2016). Dysesthesia symptoms produced by sensorimotor incongruence in healthy volunteers: An electroencephalogram study. *Journal of Pain Research* , *9* ,

1197–1204. https://doi.org/10.2147/JPR.S122564

Kida, T., Wasaka, T., Inui, K., Akatsuka, K., Nakata, H., & Kakigi, R. (2006). Centrifugal regulation of human cortical responses to a task-relevant somatosensory signal triggering voluntary movement.*NeuroImage* , *32* (3), 1355–1364. https://doi.org/10.1016/j.neuroimage.2006.05.015

Kim, J. H., & Lee, B. H. (2015). Mirror therapy combined with biofeedback functional electrical stimulation for motor recovery of upper extremities after stroke: A pilot randomized controlled trial.*Occupational Therapy International* , *22* (2), 51–60. https://doi.org/10.1002/oti.1384

Klimesch, W. (1999). EEG alpha and theta oscillations reflect cognitive and memory performance: a rKlimesch, W. (1999). EEG alpha and theta oscillations reflect cognitive and memory performance: a review and analysis. Brain Research Reviews, 29(2-3), 169–195. doi:10.1016/S016.*Brain Research Reviews* , *29* (2–3), 169–195. https://doi.org/10.1016/S0165-0173(98)00056-3

Kulkarni, B., Bentley, D. E., Elliott, R., Youell, P., Watson, A., Derbyshire, S. W. G., . . . Jones, A. K. P. (2005). Attention to pain localization and unpleasantness discriminates the functions of the medial and lateral pain systems. *European Journal of Neuroscience* , *21* (11), 3133–3142. https://doi.org/10.1111/j.1460-9568.2005.04098.x

Lee, H. M., Li, P. C., & Fan, S. C. (2015). Delayed mirror visual feedback presented using a novel mirror therapy system enhances cortical activation in healthy adults. *Journal of NeuroEngineering and Rehabilitation* , *12* (1), 1–11. https://doi.org/10.1186/s12984-015-0053-1

Light, G. A., Williams, L. E., Minow, F., Sprock, J., Rissling, A., Sharp, R., . . . Braff, D. L. (2011). Electroencephalography (EEG) and Event-Related Potentials (ERP's) with Human Participants. *Curr Protoc Nerusosci* , (619), 1–32. https://doi.org/10.1002/0471142301.ns0625s52.Electroencephalography

Lightfoot, G. (2016). Summary of the N1-P2 Cortical Auditory Evoked Potential to Estimate the Auditory Threshold in Adults. *Seminars in Hearing* , *37* (1), 1–8. https://doi.org/10.1055/s-0035-1570334

Matthys, K., Smits, M., Van der Geest, J. N., Van der Lugt, A., Seurinck, R., Stam, H. J., & Selles, R. W. (2009). Mirror-Induced Visual Illusion of Hand Movements: A Functional Magnetic Resonance Imaging Study. *Archives of Physical Medicine and Rehabilitation* ,*90* (4), 675–681. https://doi.org/10.1016/j.apmr.2008.09.571

Mccabe, C. S., Cohen, H., & Blake, D. R. (2007). Somaesthetic disturbances in fibromyalgia are exaggerated by sensory - Motor conflict: Implications for chronicity of the disease?*Rheumatology* , *46* (10), 1587–1592. https://doi.org/10.1093/rheumatology/kem204

McCabe, C. S., Haigh, R. C., Ring, E. F. J., Halligan, P. W., Wall, P. D., & Blake, D. R. (2003). A controlled pilot study of the utility of mirror visual feedback in the treatment of complex regional pain syndrome (type 1). *Rheumatology* , *42* (1), 97–101. https://doi.org/10.1093/rheumatology/keg041

McCabe, Candy S., Haigh, R. C., Halligan, P. W., & Blake, D. R. (2005). Simulating sensory-motor incongruence in healthy volunteers: Implications for a cortical model of pain. *Rheumatology* ,*44* (4), 509–516. https://doi.org/10.1093/rheumatology/keh529

Merians, A. S., Tunik, E., Fluet, G. G., Qiu, Q., & Adamovich, V. S. (2009). Innovative approaches to the rehabilitation of upper extremity hemiparesis using virtual environments. *European Journal of Physical and Rehabilitation Medicine* , *45* (1), 123–133.

Mouraux, A., Iannetti, G. D., & Plaghki, L. (2010). Low intensity intra-epidermal electrical stimulation can activate Aδ-nociceptors selectively. *Pain* , *150* (1), 199–207. https://doi.org/10.1016/j.pain.2010.04.026

Neuper, C., Wörtz, M., & Pfurtscheller, G. (2006). Chapter 14 ERD/ERS patterns reflecting sensorimotor activation and deactivation.*Progress in Brain Research* , *159* , 211–222. https://doi.org/10.1016/S0079-6123(06)59014-4

13

Nichols, T. E., & Holmes, A. P. (2001). *Nonparametric Permutation Tests for Functional Neuroimaging: A Primer with Examples .25* (August 1999), 1–25.

Nishigami, T., Nakano, H., Osumi, M., Tsujishita, M., Mibu, A., & Ushida, T. (2014). Central neural mechanisms of interindividual difference in discomfort during sensorimotor incongruence in healthy volunteers: An experimental study. *Rheumatology (United Kingdom) ,53* (7), 1194–1199. https://doi.org/10.1093/rheumatology/ket494

Northoff, G., & Bermpohl, F. (2004). Cortical midline structures and the self. *Trends in Cognitive Sciences , 8* (3), 102–107. https://doi.org/10.1016/j.tics.2004.01.004

Northoff, G., Heinzel, A., de Greck, M., Bermpohl, F., Dobrowolny, H., & Panksepp, J. (2006). Self-referential processing in our brain-A meta-analysis of imaging studies on the self. *NeuroImage ,31* (1), 440–457. https://doi.org/10.1016/j.neuroimage.2005.12.002

Numata, K., Murayama, T., Takasugi, J., Monma, M., & Oga, M. (2013). Mirror observation of finger action enhances activity in anterior intraparietal sulcus: A functional magnetic resonance imaging study.*Journal of the Japanese Physical Therapy Association ,16* (1), 1–6. https://doi.org/10.1298/jjpta.Vol16_001

Oldfield, R. C. (1971). The assessment and analysis of handedness: The Edinburgh inventory. *Neuropsychologia , 9* (1), 97–113. https://doi.org/10.1016/0028-3932(71)90067-4

Ortiz-Catalan, M., Gumundsdóttir, R. A., Kristoffersen, M. B., Zepeda-Echavarria, A., Caine-Winterberger, K., Kulbacka-Ortiz, K., . . . Hermansson, L. (2016). Phantom motor execution facilitated by machine learning and augmented reality as treatment for phantom limb pain: a single group, clinical trial in patients with chronic intractable phantom limb pain. *The Lancet , 388* (10062), 2885–2894. https://doi.org/10.1016/S0140-6736(16)31598-7

Pascual-Marqui, R. D. (2007). *Discrete, 3D distributed linear imaging methods of electric neuronal activity. Part 1: exact, zero error localization .*

Pascual-Marqui, R. D., Esslen, M., Kochi, K., & Lehmann, D. (2002). Functional imaging with low-resolution brain electromagnetic tomography (LORETA): A review. *Methods and Findings in Experimental and Clinical Pharmacology , 24* (SUPPL. C), 91–95.

Pascual-Marqui, R. D., Lehmann, D., Koenig, T., Kochi, K., Merlo, M. C. G., Hell, D., & Koukkou, M. (1999). Low resolution brain electromagnetic tomography (LORETA) functional imaging in acute, neuroleptic-naive, first-episode, productive schizophrenia.*Psychiatry Research - Neuroimaging , 90* (3), 169–179. https://doi.org/10.1016/S0925-4927(99)00013-X

Peng, K., Steele, S., Becerra, L., & Borsook, D. (2018). Brodmann area 10: Collating, integrating and high level processing of nociception and pain. *Progress in Neurobiology , 161 ,* 1–22. https://doi.org/10.1016/j.pneurobio.2017.11.004

Peng, W., Hu, Y., Mao, Y., & Babiloni, C. (2015). Widespread cortical α-ERD accompanying visual oddball target stimuli is frequency but non-modality specific. *Behavioural Brain Research , 295 ,* 71–77. https://doi.org/10.1016/j.bbr.2015.04.051

Pfurtscheller, G., & Aranibar, A. (1979). Evaluation of event-related desynchronization (ERD) preceding and following voluntary self-paced movement. *Electroencephalography and Clinical Neurophysiology ,46* (2), 138–146. https://doi.org/10.1016/0013-4694(79)90063-4

Pfurtscheller, G., & Lopes Da Silva, F. (1999, November 1). Event-related EEG/MEG synchronization and desynchronization: Basic principles. *Clinical Neurophysiology ,* Vol. 110, pp. 1842–1857. https://doi.org/10.1016/S1388-2457(99)00141-8

Pfurtscheller, G., & Neuper, C. (1994). Event-related synchronization of mu rhythm in the EEG over the cortical hand area in man.*Neuroscience Letters , 174* (1), 93–96. https://doi.org/10.1016/0304-3940(94)90127-9

Pfurtscheller, G., Neuper, C., Flotzinger, D., & Pregenzer, M. (1997). EEG-based discrimination between imagination of right and left hand movement. *Electroencephalography and Clinical Neurophysiology* ,*103* (6), 642–651. https://doi.org/10.1016/S0013-4694(97)00080-1

Price, D. D. (2000). Psychological and neural mechanisms of the affective dimension of pain. *Science* , *288* (5472), 1769–1772. https://doi.org/10.1126/science.288.5472.1769

Raichle, M. E., MacLeod, A. M., Snyder, A. Z., Powers, W. J., Gusnard, D. A., & Shulman, G. L. (2001). A default mode of brain function.*Proceedings of the National Academy of Sciences of the United States of America* , *98* (2), 676–682. https://doi.org/10.1073/pnas.98.2.676

Ramachandran, V. S., & Rodgers-Ramachandran, D. (1996). Synaesthesia in phantom limbs induced with mirrors. *Proceedings of the Royal Society B: Biological Sciences* , *263* (1369), 377–386. https://doi.org/10.1098/rspb.1996.0058

Ramachandran, V. S., Rogers-Ramachandran, D., & Cobb, S. (1995). Touching the phantom limb. *Nature* , *377* (6549), 489–490. https://doi.org/10.1038/377489a0

Rizzo, M., Petrini, L., Del Percio, C., Lopez, S., Arendt-Nielsen, L., & Babiloni, C. (2022). Mirror visual feedback during unilateral finger movements is related to the desynchronization of cortical electroencephalographic somatomotor alpha rhythms.*Psychophysiology* , (April), 1–13. https://doi.org/10.1111/psyp.14116

Rjosk, V., Kaminski, E., Hoff, M., Sehm, B., Steele, C. J., Villringer, A., & Ragert, P. (2016). Mirror visual feedback-induced performance improvement and the influence of hand dominance. *Frontiers in Human Neuroscience* , *9* (JAN2016). https://doi.org/10.3389/fnhum.2015.00702

Rusconi, E., Pinel, P., Dehaene, S., & Kleinschmidt, A. (2010). The enigma of Gerstmann's syndrome revisited: A telling tale of the vicissitudes of neuropsychology. *Brain* , *133* (2), 320–332. https://doi.org/10.1093/brain/awp281

Rusconi, E., Walsh, V., & Butterworth, B. (2005). Dexterity with numbers: rTMS over left angular gyrus disrupts finger gnosis and number processing. *Neuropsychologia* , *43* (11), 1609–1624. https://doi.org/10.1016/j.neuropsychologia.2005.01.009

Seidel, S., Kasprian, G., Furtner, J., Schöpf, V., Essmeister, M., Sycha, T., . . . Prayer, D. (2011). Mirror therapy in lower limb amputees - Alookbeyondprimary motor cortex reorganization.*Neuroradiologie* , *183* (11), 1051–1057. https://doi.org/10.1055/s-0031-1281768

Shinoura, N., Suzuki, Y., Watanabe, Y., Yamada, R., Tabei, Y., Saito, K., & Yagi, K. (2008). Mirror therapy activates outside of cerebellum and ipsilateral M1. *NeuroRehabilitation* , *23* (3), 245–252. https://doi.org/10.3233/nre-2008-23306

Thøgersen, M., Andoh, J., Milde, C., Graven-Nielsen, T., Flor, H., & Petrini, L. (2020). Individualized Augmented Reality Training Reduces Phantom Pain and Cortical Reorganization in Amputees: A Proof of Concept Study. *Journal of Pain* , *21* (11–12), 1257–1269. https://doi.org/10.1016/j.jpain.2020.06.002

Tolomeo, S., Christmas, D., Jentzsch, I., Johnston, B., Sprengelmeyer, R., Matthews, K., & Steele, J. D. (2016). A causal role for the anterior mid-cingulate cortex in negative affect and cognitive control.*Brain* , *139* (6), 1844–1854. https://doi.org/10.1093/brain/aww069

Touzalin-Chretien, P., & Dufour, A. (2008). Motor cortex activation induced by a mirror: Evidence from lateralized readiness potentials.*Journal of Neurophysiology* , *100* (1), 19–23. https://doi.org/10.1152/jn.90260.2008

Touzalin-Chretien, P., Ehrler, S., & Dufour, A. (2010). Dominance of vision over proprioception on motor programming: Evidence from ERP.*Cerebral Cortex* , *20* (8), 2007–2016. https://doi.org/10.1093/cercor/bhp271

Vladimir Tichelaar, Y. I. G., Geertzen, J. H. B., Keizer, D., & Paul Van Wilgen, C. (2007). Mirror box therapy added to cognitive behavioural therapy in three chronic complex regional pain syndrome

15

type I patients: A pilot study. *International Journal of Rehabilitation Research* ,*30* (2), 181–188. https://doi.org/10.1097/MRR.0b013e32813a2e4b

Zhang, J., & Fong, K. (2019). Enhancing mirror visual feedback with intermittent theta burst stimulation in healthy adults.*Restorative Neurology and Neuroscience* , *37* , 483–495. https://doi.org/10.3233/RNN-190927
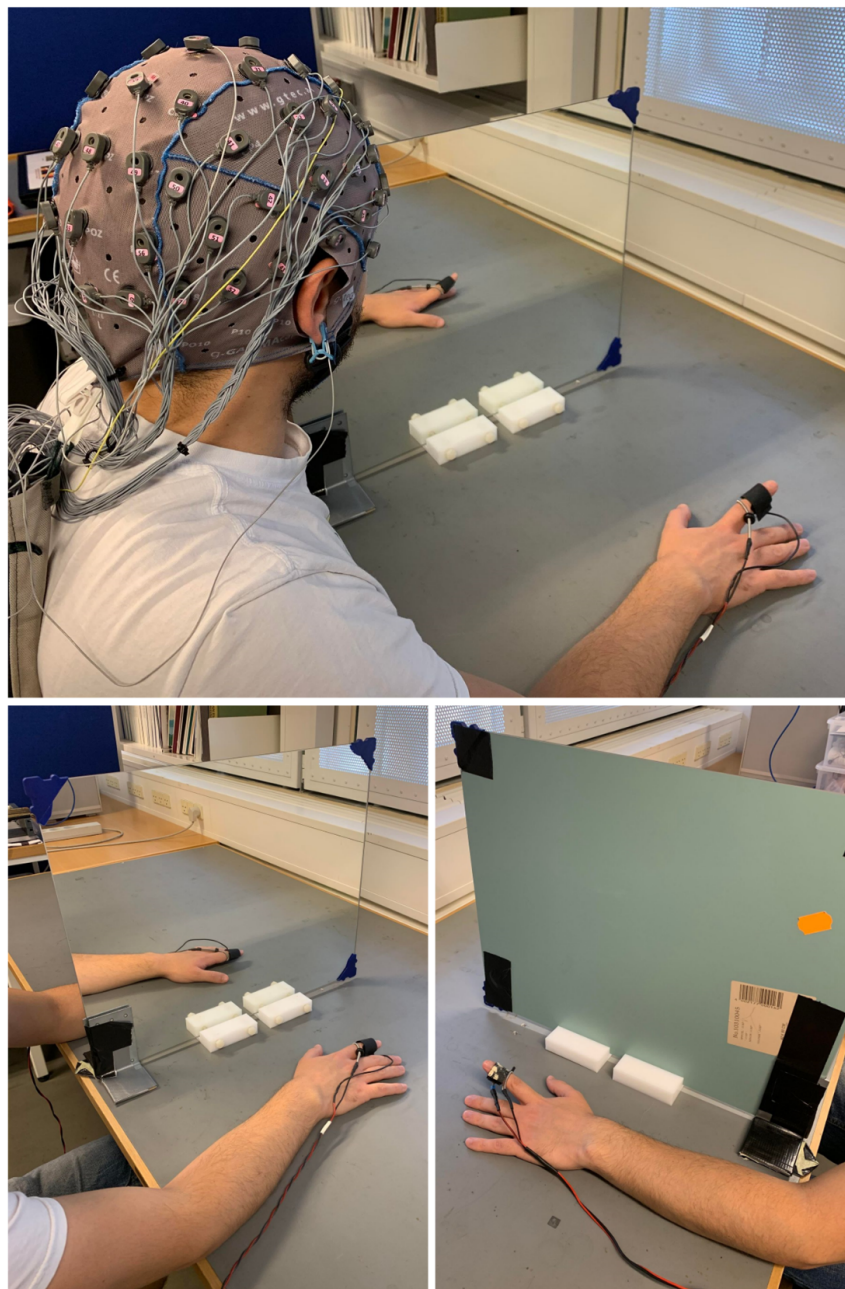
Figure 1

Figure 1

Experimental setup during the Mirror Visual Feedback (MVF) procedure (Unilateral Mirror or UM+ condition). The mirror is placed in the subjects' midsagittal plane to give the illusion of ownership of the left hand. A sham electrode was placed on the right index finger to strengthen the illusory feeling. Movements consisted of double extension (1 s approx.) with a slow release toward the table.

Figure 2
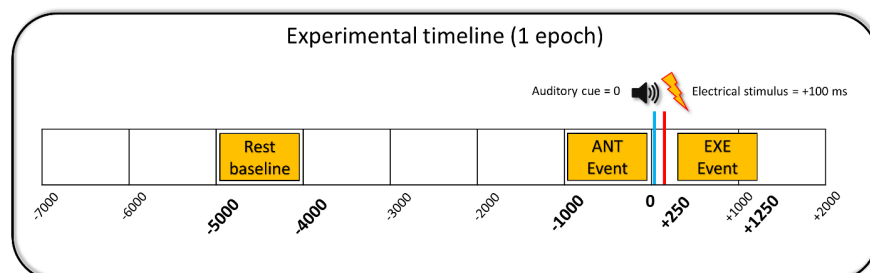
Figure 2

The figure illustrates the sequence of one trial of the experimental paradigm. In the experiment, a fixed 10 s intertrial interval was applied. During the offline analysis, 9 s epochs were extracted (from 7 s before the auditory cue to 2 s after the cue). In the figure, the time is expressed in milliseconds (ms). The 0 (zero) time corresponds to the auditory cue triggering the right index finger movement (blue line). In each trial, electrical painful stimuli were delivered on the left index finger after 100 ms from the auditory cue (red line). The anticipation (ANT) event period was defined as the time interval of 1000 ms before the 0, whereas the execution (EXE) period was defined as the time interval between 250 and 1250 ms after the 0. The alpha event-related de/synchronization (ERD/ERS) was calculated for the ANT and EXE periods in relation to a baseline period represented by the yellow box between 5000 and 4000 ms before the 0.
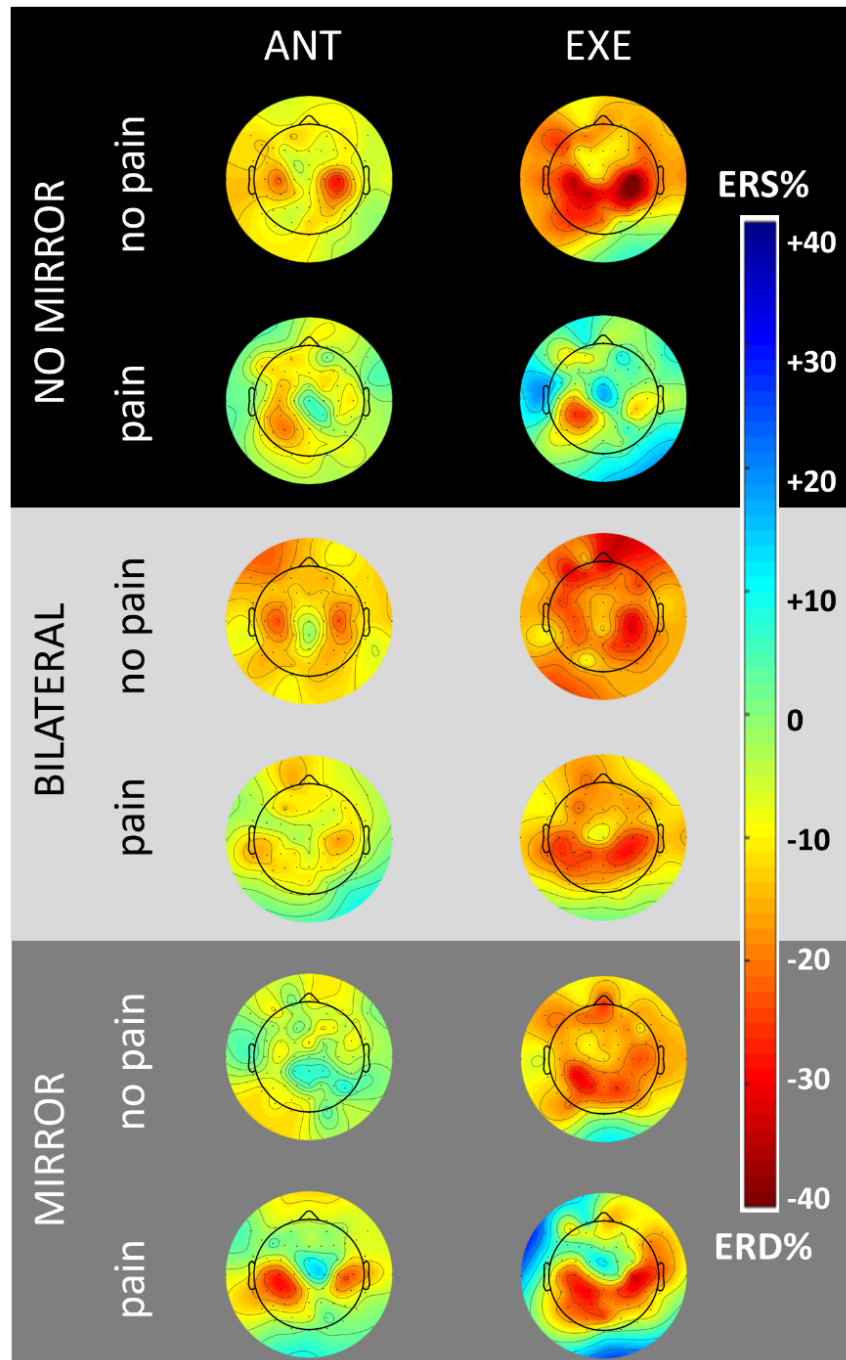
Figure 3

Figure 3

Across subjects mean 2-D maps of the alpha ERD/ERS distribution over the scalp for each condition (Unilateral No Mirror, Bilateral No Mirror, and Unilateral Mirror), phase of the event (Anticipation and Execution), and subjective perceived intensity of the stimulus (pain, no-pain). In the maps, the alpha event-related desynchronization (ERD) and synchronization (ERS) are represented with red and blue colours, respectively. Four 250 ms time windows before the auditory cue are averaged for the anticipation phase

18

(ANT). The 250 ms time windows showing the highest peak of the alpha ERD after the auditory cue are averaged for the execution phase (EXE).

Table 1

ANTICIPATION								
Conditions comparisons	BAs	Cluster size	Region	Hemisphere	MNI coordinates			T value
					x	y	z	
UM- (Pain vs No pain)	32	5 (9)	Anterior cingulate	L	-5	20	40	4.36**
	40	3 (8)	Inferior parietal lobule	L	-65	-25	20	3.95**
BM- (Pain vs No pain)	1-2-3, 4	13 (36)	Central gyrus	L/R	60	-30	45	4.61**
	40	113	Inferior parietal lobule	L/R	-65	-40	35	4.46**
	44-45	15	Inferior frontal gyrus	L/R	-60	5	15	3.36*
UM+ (Pain vs No pain)	30	2 (8)	Posterior cingulate	R	5	-55	5	-4.16**
	40	1 (5)	Inferior parietal lobule	R	40	-55	60	-4.73**
EXECUTION								
Conditions comparisons	BAs	Cluster size	Region	Hemisphere	MNI coordinates			T value
					x	y	z	
UM- (Pain vs No pain)	40	5	Inferior parietal lobule	L	-55	-25	15	3.34 n.s.
BM- (Pain vs No pain)	9-46	7 (21)	Superior frontal gyrus	R	55	15	30	4.11**
	32	7	Anterior cingulate	R	15	45	-5	3.67*
	44-45	35	Inferior frontal gyrus	R	60	15	15	3.79*
UM+ (Pain vs No pain)	10	2 (19)	Medial frontal gyrus	R	10	50	15	-4.31**
	19	5	Precuneus	R	30	-75	35	-3.87*
	24-32	2 (11)	Anterior cingulate	L/R	5	25	15	-4.66**
	39	2 (17)	Angular gyrus	R	55	-65	25	-4.75**
	40	3 (10)	Inferior parietal lobule	R	45	-55	45	-4.67**

Table 1

Voxel-based Student's t-test analysis for the eLORETA sources of the alpha ERD at the Brodmann areas (BAs) level. **Significance threshold of $p < 0.05$ corrected for multiple comparisons; *significance threshold of $p < 0.001$ uncorrected. The cluster size represents the number of voxels significant for the multiple comparisons' threshold (along with the number of voxels significant for the uncorrected threshold). The most statistically significant voxel is indicated by the Montreal Neurological Institute (MNI) coordinates. The alpha ERD is a negative percentage value indicating the reduction of power density at the event period with reference to the baseline. In the comparison between the painful vs non-painful epochs, a negative T value indicates that the alpha ERD is greater in the painful than non-painful epochs, whereas positive T values indicate that the alpha ERD is greater in the non-painful than painful epochs.
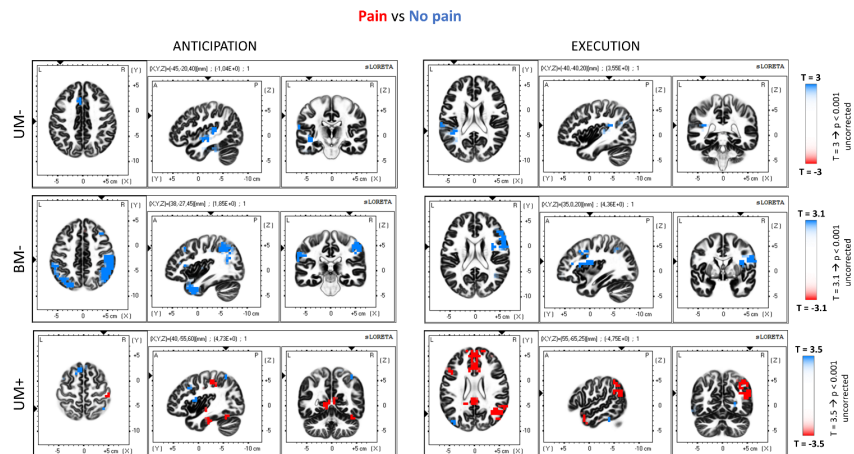
Figure 4

Pain vs **No pain**

Figure 4

Spatial distribution of the voxel-by-voxel significant p values relative to the Student's t-test for the alpha ERD/ERS eLORETA solutions. The figure illustrates the comparisons between pain and no-pain blocks for each condition (UM-, BM-, and UM+) at the anticipation and execution phase of the event. The axial, sagittal, and coronal sections are represented. The t values corresponding to the uncorrected significance threshold of p < 0.001 are shown on the right side for each condition (the t values change as the sample sizes are different among the groups). In the maps, the red voxels show the areas where the alpha ERD is significantly stronger in the painful than in no-painful blocks. Conversely, the blue voxels show the areas where the alpha ERD is significantly stronger in the no-pain than pain blocks.
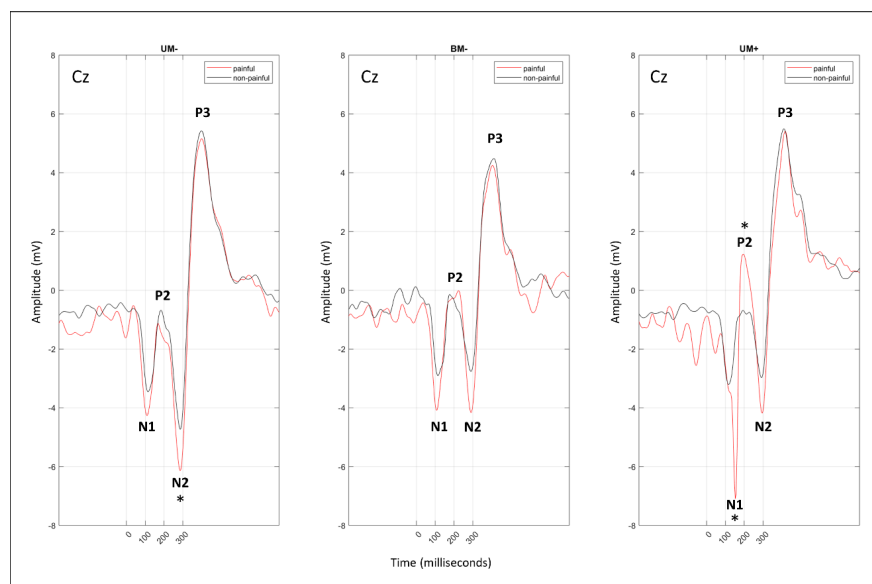
Figure 5

Figure 5

The figure illustrates the mean event-related potentials (ERPs) generated in response to auditory cues and

20

electrical sensory stimuli at the Cz electrode. The difference between painful (red line) and non-painful (black line) blocks are represented for each condition (UM-, BM-, and UM+). Statistical analysis (which one? T-test?) showed significant differences in the N2 peak for the UM- condition as well as in the N1 and P2 peaks for the experimental UM+ condition (*p < 0.05).
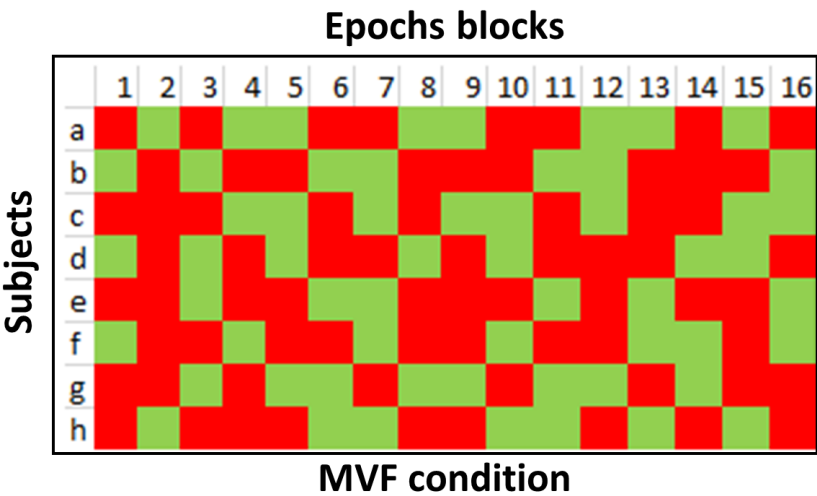
Figure 6

Figure 6

The graph shows the distribution of the blocks where each subject (Y-axis) perceived the stimuli as painful (NRS > 5, red blocks) or non-painful (NRS < 5, green blocks) in the experimental Unilateral Mirror (UM+) condition. Each block consisted of 5 trials. Therefore, a total of 16 blocks are shown on the X-axis. The RUNS test showed as the red and green blocks are randomly distributed for each subject (p < 0.05).
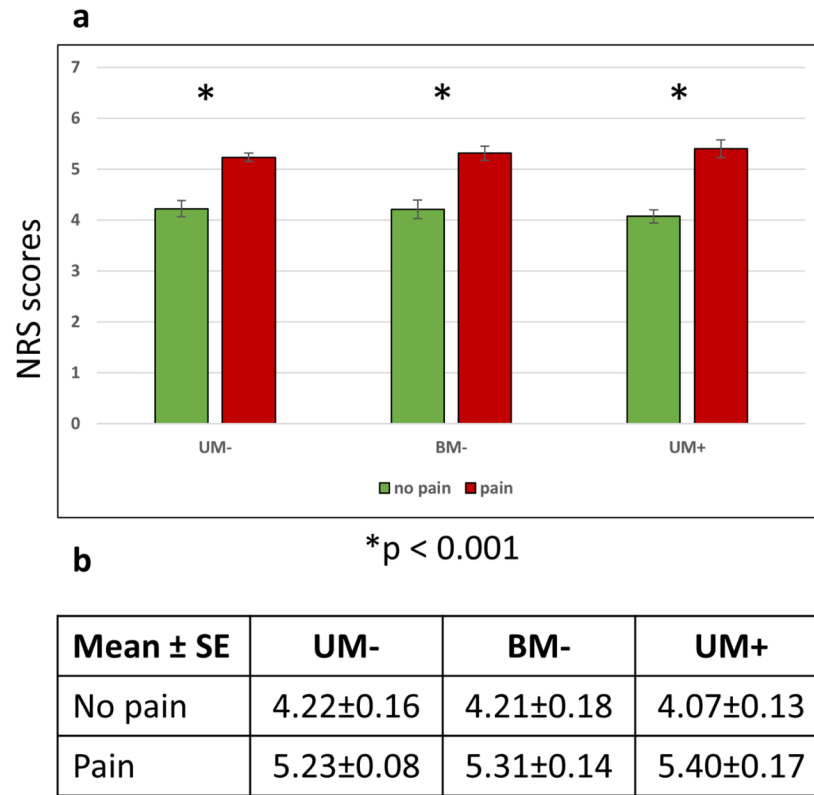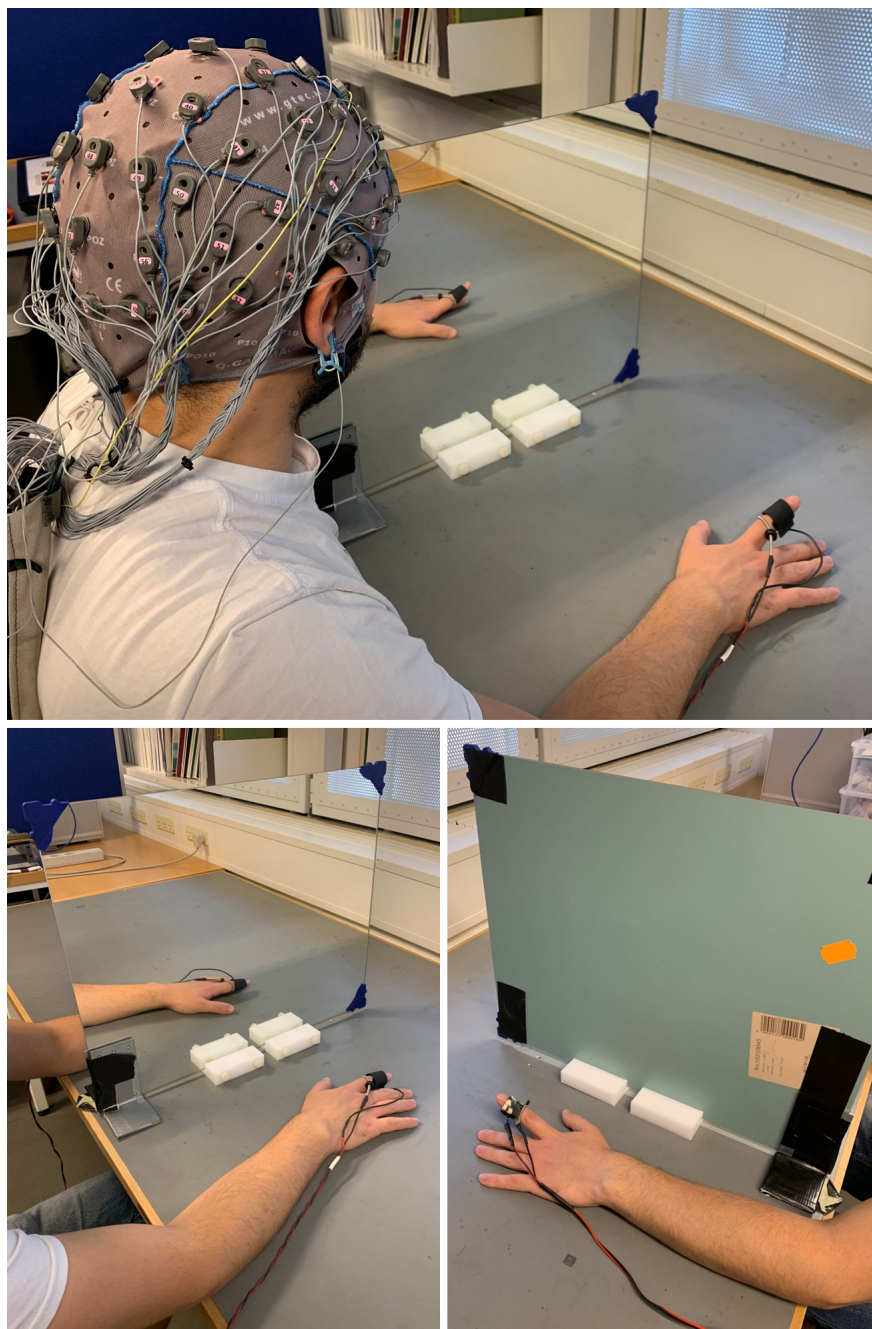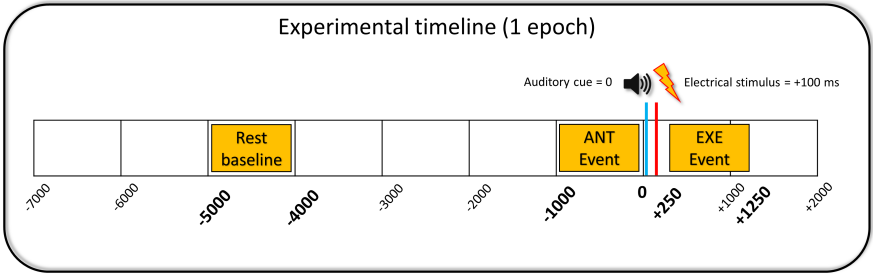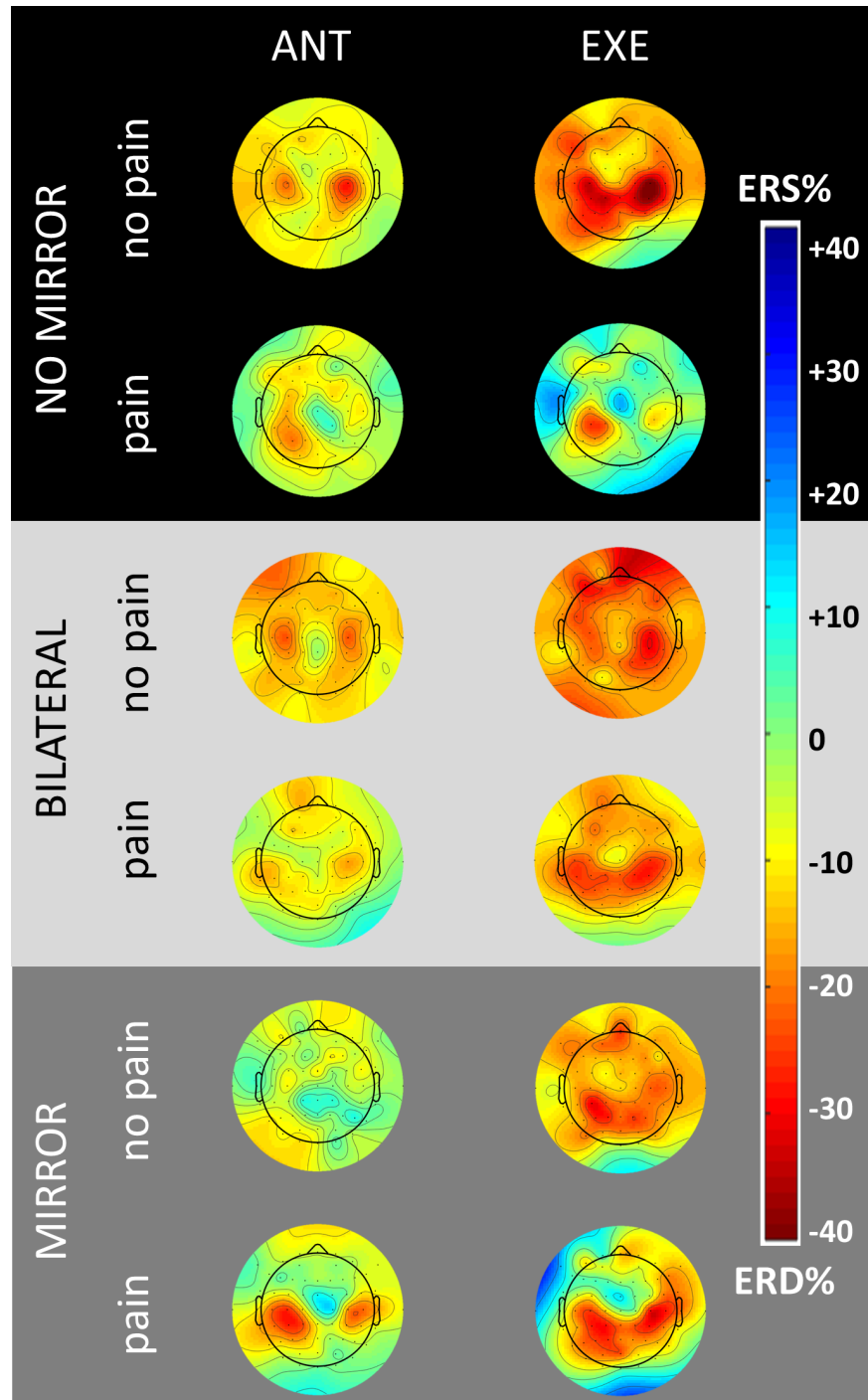
Figure 7

a

b

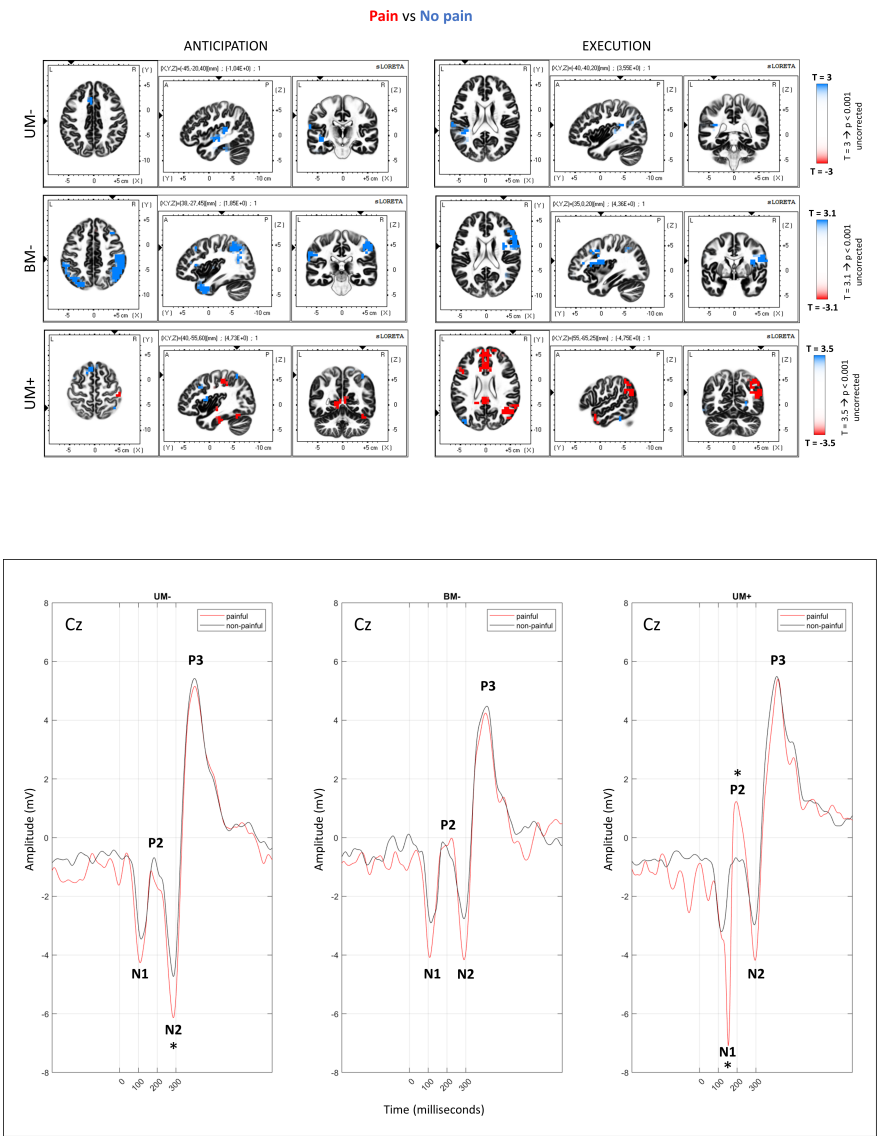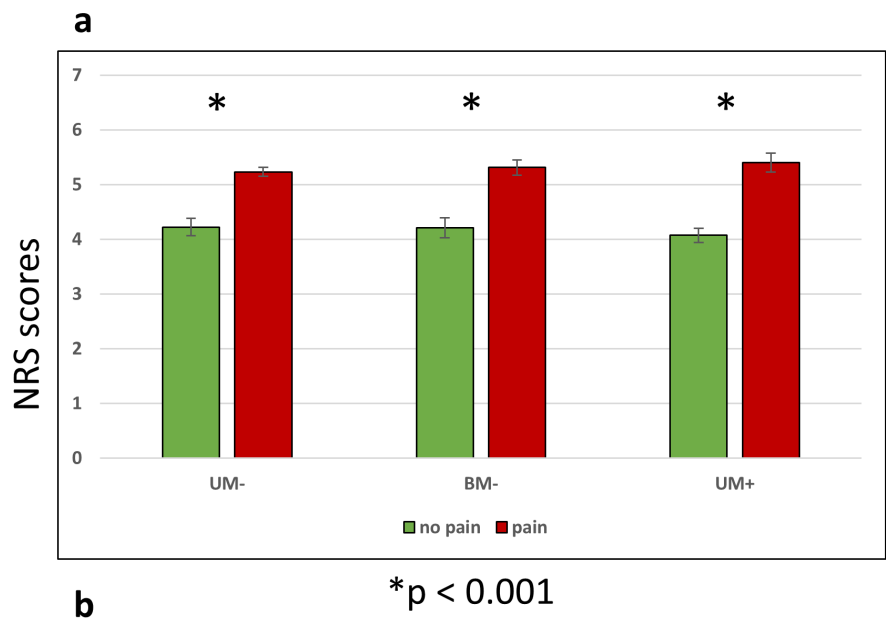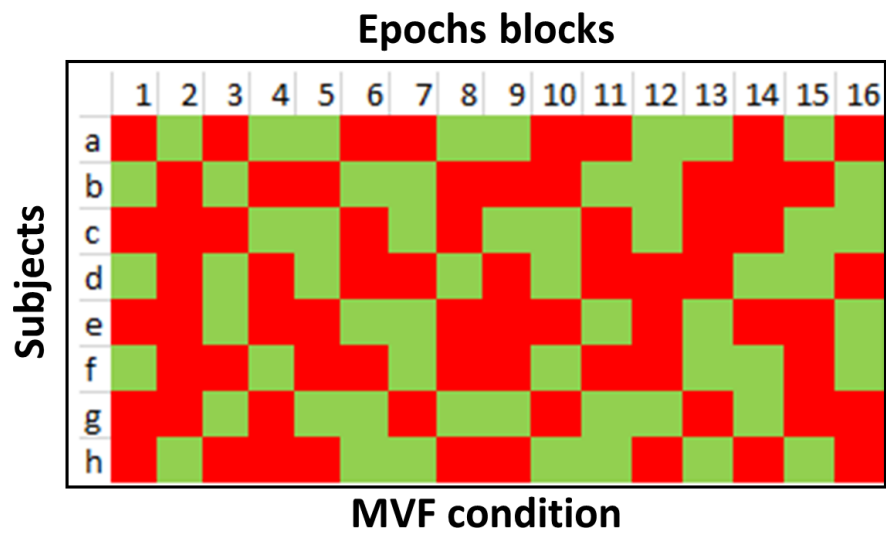| Mean ± SE	UM-	BM-	UM+
No pain	4.22±0.16	4.21±0.18	4.07±0.13
Pain	5.23±0.08	5.31±0.14	5.40±0.17

Figure 7

Histograms of the average of the Numerical Rating Scale (NRS) values provided by the subjects during each condition (a). The ratings were separated into painful (NRS > 5, red) and non-painful (NRS < 5, green). Paired samples t-tests controlled that the painful and non-painful ratings were significantly different in each condition (p < 0.001). The table below (b) shows the mean and the standard error (SE) for each condition and perceived intensity.

Experimental timeline (1 epoch)

Auditory cue = 0

Electrical stimulus = +100 ms

| | | Rest baseline | | | | ANT Event | | EXE Event | |

-7000 -6000 **-5000** **-4000** -3000 -2000 **-1000** **0** **+250** +1000 **+1250** +2000

Pain vs **No pain**

ANTICIPATION   EXECUTION

Epochs blocks

MVF condition

a

*p < 0.001

b

Mean ± SE	UM-	BM-	UM+
No pain	4.22±0.16	4.21±0.18	4.07±0.13
Pain	5.23±0.08	5.31±0.14	5.40±0.17

ANTICIPATION								
Conditions comparisons	BAs	Cluster size	Region	Hemisphere	MNI coordinates			T value
					x	y	z	
UM-	32	5 (9)	Anterior cingulate	L	-5	20	40	4.36**
(Pain vs No pain)	40	3 (8)	Inferior parietal lobule	L	-65	-25	20	3.95**
BM-	1-2-3, 4	13 (36)	Central gyrus	L/R	60	-30	45	4.61**
(Pain vs No pain)	40	113	Inferior parietal lobule	L/R	-65	-40	35	4.46**
	44-45	15	Inferior frontal gyrus	L/R	-60	5	15	3.36*
UM+	30	2 (8)	Posterior cingulate	R	5	-55	5	-4.16**
(Pain vs No pain)	40	1 (5)	Inferior parietal lobule	R	40	-55	60	-4.73**

EXECUTION								
Conditions comparisons	BAs	Cluster size	Region	Hemisphere	MNI coordinates			T value
					x	y	z	
UM-	40	5	Inferior parietal lobule	L	-55	-25	15	3.34 n.s.
(Pain vs No pain)								
BM-	9-46	7 (21)	Superior frontal gyrus	R	55	15	30	4.11**
(Pain vs No pain)	32	7	Anterior cingulate	R	15	45	-5	3.67*
	44-45	35	Inferior frontal gyrus	R	60	15	15	3.79*
	10	2 (19)	Medial frontal gyrus	R	10	50	15	-4.31**
	19	5	Precuneus	R	30	-75	35	-3.87*
UM+	24-32	2 (11)	Anterior cingulate	L/R	5	25	15	-4.66**
(Pain vs No pain)	39	2 (17)	Angular gyrus	R	55	-65	25	-4.75**
	40	3 (10)	Inferior parietal lobule	R	45	-55	45	-4.67**